DAMAGE MODELLING OF THIN-PLY NANO-REINFORCED COMPOSITE LAMINATES

Carolina Furtado[1,2,4], Xinchen Ni[3], Estelle Kalfon-Cohen[3,4], Albertino Arteiro[1,2], Brian L. Wardle[4] and Pedro P. Camanho[1,2]

[1] DEMec, Faculdade de Engenharia da Universidade do Porto, Rua Dr. Roberto Frias, s/n, 4200-465 Porto, Portugal
[2] INEGI, Instituto de Ciência e Inovação em Engenharia Mecânica e Engenharia Industrial, Rua Dr. Roberto Frias, 400, 4200-465 Porto, Portugal
[3] Department of Mechanical Engineering, Massachusetts Institute of Technology, 77 Massachusetts Avenue, Cambridge, MA 02139, United States
[4] Department of Aeronautics and Astronautics, Massachusetts Institute of Technology, 77 Massachusetts Avenue, Cambridge, MA 02139, United States

Keywords: Finite elements, Continuum damage mechanics, Fracture mechanics, Carbon nanotubes, Carbon fiber composites

ABSTRACT

Composite laminates composed of unidirectional carbon fibre-epoxy plies nano-stitched together with vertically aligned carbon nanotube arrays (A-CNT) have been recently developed. This technology has proven to improve both interlaminar and intralaminar composite strength and toughness. The consequences of nanostitching interfaces has mainly been studied by measuring the Interlaminar shear strength (ILSS) of nanostitched interfaces and the respective baseline configurations of the same material system using short beam shear tests. In this study, short beam shear tests of unreinforced and nanostitched samples are modelled to better understand what are the effects of this type of nano-reinforcement on the mechanics of fracture of composite materials. Intralaminar damage is simulated using a continuum damage model previously proposed in the literature [1]–[3]. Interlaminar damage was simulated using a cohesive zone model implemented in ABAQUS. It was considered that the inclusion of carbon nanotubes in the interfaces leads to an increase of mode I and mode II fracture toughnesses. Since the enhancement factor was unknown, the fracture toughness of reinforced interfaces was inversely identified by analyzing the damage propagation and load displacement curves predicted by the models. The numerical results suggest that the nanostitched interfaces are ~5% or ~10-15% tougher than unreinforced interfaces depending on the carbon fibre-epoxy material system used.

1 INTRODUCTION

Interest has been growing in the development of nanostructured composite materials, in which nanoparticles such as carbon nanotubes are used alongside microscale fibre composite laminates. The main idea behind the combination is to improve the matrix dominated properties of traditional composites. In fact, carbon nanotubes introduce additional energy dissipation mechanisms that could enhance the toughness of the matrix and therefore be used to improve the interfacial and transverse properties of composite laminates.

The combination of carbon nanotubes into composite laminates has mainly been attempted by either adding them to the matrix, to the interfaces or to attach them directly in the fibres. To mitigate the processing problems associated with the impregnation of nano-modified resins and to further improve the mechanical performance of nano-engineered composite materials, advanced methods have been developed to incorporate nanotubes as through the thickness reinforcement. [4]–[8]

Recently, composite laminates composed of carbon fibre-epoxy plies nano-stitched together with vertically aligned carbon nanotube arrays have been developed. A schematic representation of the concept is shown in figure 1. It has been shown that this innovative process guarantees a good dispersion

of carbon nanotubes and improves both interlaminar [9]–[11] and intralaminar [12] composite strength and toughness and significantly increases the electrical and thermal conductivity, allowing the possibility of creating not only a new generation of mechanically enhanced composite materials but also of multifunctional structures [9], [12], [13].

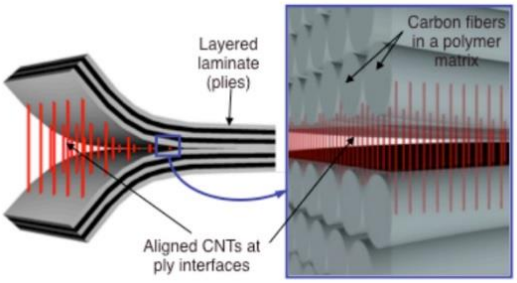

Figure 1: Schematic representation of a nanostitched composite interface [9].

Lewis [10] and Ni et al. [14] performed short beam shear tests to study the influence of nanostitching on the Interlaminar shear strength (ILSS) in two material systems. In the first study [10], IM7/8552 quasi isotropic laminate reinforced with 5-65μm CNT in every interface were tested. Even though samples with seven different CNT heights were tested, no relevant difference is shown between the experimental results for the reinforced samples because regardless of the initial height, the forests were compressed to around 5μm in the interface. The average improvement in ILSS over the unreinforced baseline was 8.75±0.5%. Ni et al. [14] tested an AS4/8552 quasi isotropic laminate reinforced with 20μm CNT in every interface and observed no statistically significant improvement between baseline and nanostitched specimens.

Following Lewis [10] and Ni [14], Cohen et al. [15] performed short beam shear tests on a nanostitched quasi-isotropic thin-ply laminate and compared its performance with the performance of unreinforced conventional grade laminates and thin-ply material. The goal of this experimental campaign was to assess the advantages combining thin-ply laminates with nano-stitched interfaces based on carbon nanotubes.

The work presented in this paper serves as a complementary study to the work presented in refs. [14] and [15]. The short beam shear tests are simulated using the modelling strategy presented in section 2 to better understand the toughening effects of the inclusion of CNTs in the interfaces of carbon-epoxy laminates.

2 MODELLING STRATEGY

The simulation of damage in composite laminates requires the use of models that are able to capture intralaminar (matrix cracking, fibre fracture) and interlaminar (delamination) damage. The constitutive models used in this work to simulate interlaminar damage, interlaminar damage and the finite element model used in this work are presented in this section.

2.1 Intralaminar damage

In this work, intralaminar damage is simulated using the continuum damage model proposed by Maimí et al. [1]–[3]. The model was developed to predict the onset and accumulation of intralaminar damage mechanisms (matrix cracking and fibre fracture) in laminated composites. The continuum damage model was defined in the framework of the thermodynamics of irreversible processes. Generally speaking, the formulation of the continuum damage models starts by the definition of a potential (the complementary free energy density) as a function of damage variables, which is the basis for establishing the relation between the stress and the strain tensors. More details on the continuum damage model can be found in refs. [1]–[3].

Proper model formulation is clearly fundamental to accurately predict damage propagation in composite laminates, however the material properties used to feed the model also have to be accurately determined and used. The authors consider that it is particularly important to take into account that the ply strengths are *in-situ* properties, i.e. are a function of the ply thickness and ply position in a

multidirectional laminate. [16]

2.2 Interlaminar damage

As a first approach, and to access the accuracy of the methodology, interlaminar damage was simulated using the cohesive zone model implemented in ABAQUS [17]. For nanostitched interfaces, this is a simplification since these models were not developed accounting for the inelastic deformation and fracture on nano-reinforced interfaces. In the future, such cohesive zone models should be developed based on cohesive laws identified using analytical models supported by experimental findings and the simulations should be rerun.

The constitutive behaviour of cohesive elements is implemented using a cohesive zone model that relates the tractions, τ, to the displacement jumps, Δ, at the interfaces where crack propagation occurs. The initial response of the cohesive element is assumed to be linear until damage initiation. ABAQUS allows the definition of different damage initiation and progration criteria. Damage initiation is related to the interfacial strength of the material and damage propagation is related to the rate at which the material stiffness is degraded after the initiation criterion is reached [17]. In this work, the quadratic nominal stress criterion was used for damage initiation and the Benzeggagh-Kenane fracture criterion was used for damage propagation [18].

Cohesive finite elements require very refined meshes: the fracture process zone should include at least 3 cohesive elements so that delamination is accurately simulated. Turon et al. [19] proposed an engineering solution to avoid the use of such refined meshes that consists lowering the cohesive strengths whilst keeping the fracture toughness constant to enlarge the cohesive zone and to enable a better representation of the softening behaviour at the vicinity of the crack tip. Turon et al. [19], suggested that the effective strength in pure mode I should be given by

$$\tau_N = min(Y_T^{UD}, \overline{\tau_N})$$

where Y_T^{UD} is the transverse tensile strength, and $\overline{\tau_N}$ is given by

$$\overline{\tau_N} = \sqrt{\frac{9\pi E G_{Ic}}{32 N_e l_e}}$$

N_e is the number of elements in the cohesive zone that should be at least 3, l_e is the element size in the direction of crack propagation, and G_{Ic} is the mode I fracture toughness. Turon et al. [20] demonstrated that changes in the local mode ratio during the evolution of damage during mixed mode loading might lead to erroneous calculation of the energy dissipation. For this reason, the shear strength should not be a fully independent material property, but rather a function of the fracture toughness and of the normal strength:

$$\tau_{sh} = \tau_N \sqrt{\frac{G_{IIc}}{G_{Ic}}}$$

where G_{Ic} and G_{IIc} are the mode I and mode II fracture toughness, respectively. The penalty stiffness used was 10^6 N/mm^3 [21].

2.3 Finite Element Model

The simulation of the short beam shear tests performed by Ni et al. [11] and Cohen et al. [12] was performed to better understand the consequences of reinforcing the interfaces with carbon nanotubes. The model is composed by i) two lower supports composed of C3D8r elastic elements, ii) a loading nose composed of C3D8r elastic elements and iii) the laminate. One user material C3D8r finite element per ply is used to simulate intralaminar damage and the plies are connected by 0.01mm thick COH3D8 cohesive element. The supports and loading nose are also simulated to avoid unrealistic damage development on the outer layers and because their dimensions are not negligible compared to the dimensions of the specimens. The bottom of the supports are clamped and a smooth step with amplitude of 0.4 mm is applied to the top of the loading nose as shown in figure 3. Frictionless contact is defined between every element to avoid interpenetration. A mesh of 0.25x0.25xt mm^3 is used for the ply

elements and 0.25x0.25x0.01 mm^3 for the cohesive elements. The mesh and boundary conditions used are shown in figure 3.

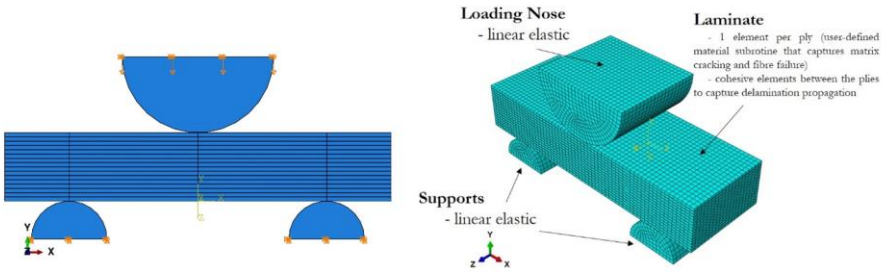

Figure 3: Boundary conditions (left) and mesh (right) used to simulate the SBS specimen.

3 NUMERICAL RESULTS

3.1 Numerical results for SBS in AS4/8552 CFRP

Ni et al. [14] tested two sets of short beam shear samples following the ASTM D2344 standard: the baseline samples that are not reinforced in the interfaces and the reinforced samples that are nanostitched with carbon nanotubes in every interface. The samples were manufactured from 147gsm AS4/8552 carbon/epoxy. The layup used was $[0/90/45/-45]_{2s}$. The experimental results are shown in table 1.

Even though Ni et al. [14] found no statistically difference between ILSS of the baseline and nanostitched samples, it was considered that the inclusion of carbon nanotubes in the interfaces increases the mode I and mode II fracture toughnesses as suggested in refs. [9], [11]. Since the effective enhancement factor is not known, 3 simulations were performed to inversely identify G_{Ic} and G_{IIc} and to understand what the consequences of the toughening are. These simulations are identified as AS4-CNT-5, AS4-CNT-10 and AS4-CNT-15. The mode I and mode II fracture toughnesses used are shown in table 1. As done in Ref. [22] in the absence of the fracture toughness values for AS4/8552 carbon/epoxy system, the properties previously measured for IM7/8552 are used.

Reference	Assumed enhancement factor	G_{Ic} [kJ/m^2]	G_{IIc} [kJ/m^2]	σ^{Exp} [MPa]	SE [MPa]	σ^{Num} [MPa]	Diference (%)
AS4-REF	-	0,28 [22]	0,79 [22]	94,99 [14]	1.19 [14]	97,48	2,6
AS4-CNT-5	5%	0,29	0,83	96,24 [14]	0.92 [14]	102,24	6,2
AS4-CNT-10	10%	0,31	0,87	96,24 [14]	0.92 [14]	103,07	7,1
AS4-CNT-15	15%	0,32	0,91	96,24 [14]	0.92 [14]	103,74	7,8

Table 1: SBS model and experimental results for AS4/8552 $[0/90/45/-45]_{2s}$ specimens. SE is standard error.

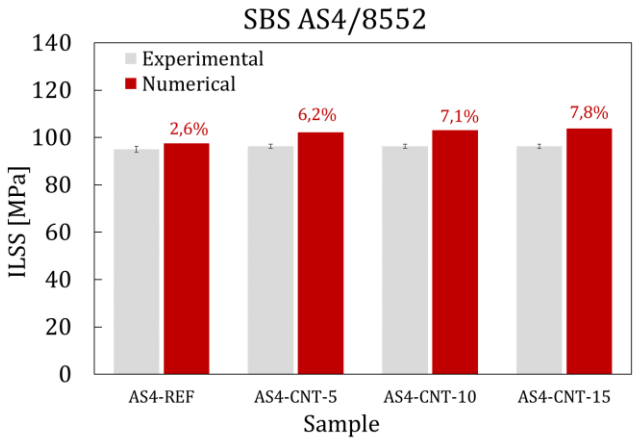

Figure 4: SBS model and experimental results for AS4/8552 $[0/90/45/-45]_{2s}$ specimens as a function of assumed toughness increase due to A-CNTs.

As shown in figure 4, the ILSS does not increase proportionally to the increase in fracture toughness increase. The numerical results suggest that the inclusion of CNTs lead to an increase in mode I and mode II fracture toughness around or lower than 5%. For this reason, AS4-REF and AS4-CNT-5 simulations are analysed in more detail in Figure 5 which shows the load displacement curves and the damage progression for these simulations. To simplify the analysis, only highly damaged elements (damage variable higher than 0.9) are shown. Damage progression is very similar for both specimens, even though for AS4-CNT-5 damage develops for higher applied displacements:

- **A** - damage develops on the top interface, below the loading nose
- **B** - damage develops towards the centre of the specimen.
- **C** - the specimen fails. Large interlaminar cracks that propagate through the specimen's length and width appear near the middle interfaces. Some matrix cracks are also visible.

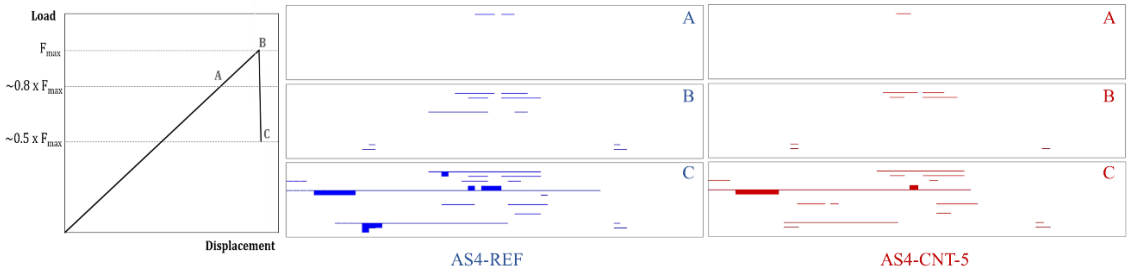

Figure 5: Predicted load-displacement curves and damage progression for AS4-REF and AS4-CNT-5 samples in SBS.

3.2 Numerical results for SBS in HTS40/Q-1112 CFRP

Cohen et al. [15] used 54gsm HTS40/Q-1112 carbon/epoxy material system to manufacture four sets of short beam shear samples:

- **Thin-REF:** un-reinforced quasi-isotropic $([0/90/\pm45]_6)_s$ thin ply samples
- **Thin-CNT:** quasi-isotropic $([0/90/\pm45]_6)_s$ thin ply samples nanostitched in the middle 15 interfaces
- **Thick-REF:** un-reinforced quasi-isotropic $([0_3/90_3/\pm45_3]_2)_s$ samples
- **Thick-CNT:** quasi-isotropic $([0_3/90_3/\pm45_3]_2)_s$ samples nanostitched in the middle 5 interfaces.

The samples were manufactured and tested following the ASTM D2344 standard. The goal of this experimental campaign was to understand the consequences nanostitching has when combined with thin-ply laminates and what are the improvements on interlaminar strength and toughness that can be obtained compared to the baseline material. Cohen et al. [15] analyzed the broken samples and reported that the major cracks of the thin-ply nanostitched samples (Thin-CNT) were located on unreinforced interfaces, away from the midplane of the samples. Unlike the reinforced samples, the major cracks of the baseline samples (Thin-REF and Thick-REF) were located near the midplane. This suggests that the presence of the CNTs leads to an increase in interlaminar fracture toughness. This is particularly noticeable for the thin-ply configuration.

Since most of the material properties needed to simulate intralaminar and interlaminar damage are unknown for the HTS40/Q-1112 carbon/epoxy material system at this point of the work, only a qualitative analysis was made for this material. The material properties used are not relevant since the goal is not to get accurate predictions of the load displacement curve and ILSS but rather to better understand the differences in damage propagation of the four configurations. In the simulations of the unreinforced samples (Thick-REF and Thin-REF) the fracture toughness of the elements in every interface are the same. However, since the middle 5 and middle 15 interfaces are reinforced for the nanostitched samples (Thick-CNT and Thin-CNT, respectively), the fracture toughness of the elements on those interfaces are increased. Since the toughening factor induced by the presence of the CNTs is

not known, two enhancement factors were used: 5% and 10%. A summary of the simulations performed are shown in table 2.

Reference	Layup	Nanostitched interfaces	Assumed enhancement factor	G_{Ic} [kJ/m^2]	G_{IIc} [kJ/m^2]
Thick-REF	$([0_3/90_3/\pm45_3]_2)_s$	None	-	G_{Ic}	G_{IIc}
Thick-CNT-10	$([0_3/90_3/\pm45_3]_2)_s$	Middle 5 interfaces	10%	1.10 x G_{Ic}	1.10x G_{IIc}
Thick-CNT-15	$([0_3/90_3/\pm45_3]_2)_s$	Middle 5 interfaces	15%	1.15 x G_{Ic}	1.15x G_{IIc}
Thin-REF	$([0/90/\pm45]_6)_s$	None	-	G_{Ic}	G_{IIc}
Thin-CNT-10	$([0/90/\pm45]_6)_s$	Middle 15 interfaces	10%	1.10 x G_{Ic}	1.10x G_{IIc}
Thin-CNT-15	$([0/90/\pm45]_6)_s$	Middle 15 interfaces	15%	1.15 x G_{Ic}	1.15x G_{IIc}

Table 2: Characteristics of the HTS40/Q-1112 SBS simulations.

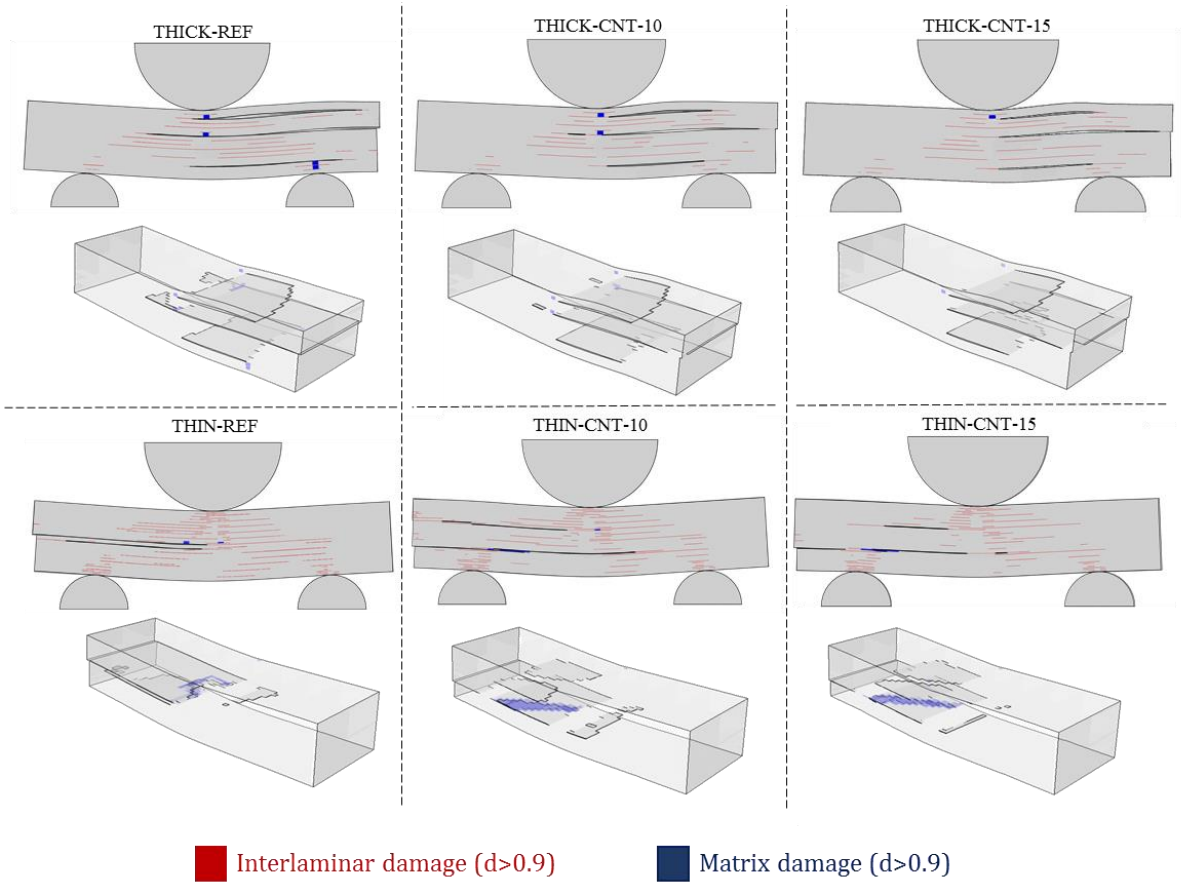

Figure 6: Predicted damage after breaking. Discontinuities are delamination planes. Matrix damage and interlaminar damage are shown in blue and red, respectively.

Figure 6 shows the predicted extension of damage after breaking. Even though the model also predicts the extension of the subcritical damage, only highly damaged elements (damage variable higher than 0.9) are shown to make the analysis simpler. Both the Thick-REF and Thin-REF simulations predict a large extension of damage through the thickness of the sample, with the major cracks in the middle or near the middle interfaces. As shown in figure 6, for the thin-ply material, an increase of 10%-15% on the fracture toughness of the middle interfaces is enough to shift the damage away from the centre. For this configuration, for an increase in fracture toughness as low as 10%, the middle reinforced region starts acting as an elastic region and therefore, all the simulations predict a similar behaviour regardless of the enhancement factor used. Contrary to the thin configuration, the damage mode is very similar for the standard grade reinforced and unreinforced samples (Thick-REF, Thick -CNT-10 and Thick -CNT-

15). For conventional thickness material, small increases on the fracture toughness are not sufficient to change the failure mode and the failing interfaces. For the standard grade configurations, the enhancement factor could be determined by comparing the numerical and experimental ILSS, as explained in section 3.1. To do so, the material properties of the HTS40/Q-1112 carbon-epoxy system should be determined. However, since the same material is used to manufacture the Thin and Thick configurations, it is plausible that the enhancement factor is in the same order of magnitude. In general, the damage extension agrees with the experimental data reported by Cohen et al. [15]:

- **Thin-REF:** clear interlaminar crack in the middle of the sample
- **Thin-CNT:** clear interlaminar crack in the unreinforced interface closest to the mid plane
- **Thick-REF:** large number of interlaminar cracks, being the major ones in the near the middle interface
- **Thick-CNT:** large number of interlaminar cracks, being the major ones in the near the middle interface.

4 CONCLUSIONS

In this study, modelling of short beam shear tests of unreinforced and nanostitched samples is performed to better understand what are the consequences of reinforcing the interfaces with carbon nanotubes. The numerical results suggest that the nanostitched interfaces need be no larger than 5% tougher than unreinforced interfaces to match the experimental results. In this work, interlaminar damage in the nanostitched interfaces was simulated using the cohesive zone model developed for unreinforced interfaces. This is a simplification and the simulation of nano-modified interfaces should be addressed with more detail. The cohesive laws for nanostitched interfaces should be determined experimentally. This information will allow the comparison of the fracture toughness by means of the crack resistant curve and support the development of analysis methods to predict inelastic deformation and fracture on nano-reinforced interfaces.

ACKNOWLEDGEMENTS

This work was funded by National Funds through FCT – Fundação para Ciência e a Tecnologia in the scope of project MITP-TB/PFM/0005/2013. The first, third, fourth, fifth and sixth authors would like to thank FCT for the financial support. The first author would also like to thank Fulbright for the financial.

This work was supported by Airbus, Embraer, Lockheed Martin, Saab AB, Hexcel, Saertex, TohoTenax, and ANSYS through MIT's Nano-Engineered Composite aerospace STructures (NECST) Consortium.

REFERENCES

[1] P. Maimí, P. P. Camanho, J. A. Mayugo, and C. G. Dávila, "A continuum damage model for composite laminates: Part I – Constitutive model," *Mech. Mater.*, vol. 39, no. 10, pp. 897–908, 2007.

[2] P. Maimí, P. P. Camanho, J. A. Mayugo, and C. G. Dávila, "A continuum damage model for composite laminates: Part II – Computational implementation and validation," *Mech. Mater.*, vol. 39, no. 10, pp. 909–919, 2007.

[3] P. Maimí, "Modelización constitutiva y computacional del daño y la fractura de materiales compuestos," Universitat de Girona, 2007.

[4] M. Arai, Y. Noro, K. Sugimoto, and M. Endo, "Mode I and mode II interlaminar fracture toughness of CFRP laminates toughened by carbon nanofiber interlayer," *Compos. Sci. Technol.*, vol. 68, no. 2, pp. 516–525, 2008.

[5] H. Qian, A. Bismarck, E. S. Greenhalgh, and M. S. P. Shaffer, "Carbon nanotube grafted carbon fibres: A study of wetting and fibre fragmentation," *Compos. Part A Appl. Sci. Manuf.*, vol. 41, no. 9, pp. 1107–1114, 2010.

[6] F. An, C. Lu, J. Guo, S. He, H. Lu, and Y. Yang, "Preparation of vertically aligned carbon

nanotube arrays grown onto carbon fiber fabric and evaluating its wettability on effect of composite," *Appl. Surf. Sci.*, vol. 258, no. 3, pp. 1069–1076, 2011.

[7] R. J. Sager, P. J. Klein, D. C. Lagoudas, Q. Zhang, J. Liu, L. Dai, and J. W. Baur, "Effect of carbon nanotubes on the interfacial shear strength of T650 carbon fiber in an epoxy matrix," *Compos. Sci. Technol.*, vol. 69, no. 7, pp. 898–904, 2009.

[8] E. J. Garcia, B. L. Wardle, A. John Hart, and N. Yamamoto, "Fabrication and multifunctional properties of a hybrid laminate with aligned carbon nanotubes grown In Situ," *Compos. Sci. Technol.*, vol. 68, no. 9, pp. 2034–2041, 2008.

[9] E. J. Garcia, B. L. Wardle, and A. John Hart, "Joining prepreg composite interfaces with aligned carbon nanotubes," *Compos. Part A Appl. Sci. Manuf.*, vol. 39, no. 6, pp. 1065–1070, 2008.

[10] D. J. Lewis, "Interlaminar Reinforcement of Carbon Fiber Composites from Unidirectional Prepreg Utilizing Aligned Carbon Nanotubes," Massachusetts Institute of Technology, 2016.

[11] B. G. Falzon, S. C. Hawkins, C. P. Huynh, R. Radjef, and C. Brown, "An investigation of Mode I and Mode II fracture toughness enhancement using aligned carbon nanotubes forests at the crack interface," *Compos. Struct.*, vol. 106, pp. 65–73, 2013.

[12] R. Guzman de Villoria, P. Hallander, L. Ydrefors, P. Nordin, and B. L. Wardle, "In-plane strength enhancement of laminated composites via aligned carbon nanotube interlaminar reinforcement," *Compos. Sci. Technol.*, vol. 133, pp. 33–39, 2016.

[13] D. Lewis and B. L. Wardle, "Interlaminar shear strength investigation of aligned carbon nanotube-reinforced prepreg composite interfaces," *56th AIAA/ASCE/AHS/ASC Struct. Struct. Dyn. Mater. Conf.*, no. January, pp. 2–6, 2015.

[14] X. Ni, E. Cohen, C. Furtado, R. Kopp, N. Fritz, A. Arteiro, G. Valdes, T. Hank, G. Bostnar, M. N. Mavrogadro, S. M. Spearing, P. P. Camanho, and B. L. Wardle, "Interlaminar Reinforcement Of Carbon Fiber Composites Using Aligned Carbon Nanotubes," in *The 21st lnternational Composites Conference on Composite Materials*, 2017.

[15] E. Kalfon-Cohen, R. Kopp, X. Ni, N. Fritz, C. Furtado, A. Arteiro, G. Borstnar, M. N. Mavrogordato, S. M. Spearing, P. P. Camanho, and B. L. Wardle, "Synergetic Effects of Thin Ply and Nanostitching Studied by Synchrotron Radiation Computed Tomography," in *The 21st lnternational Composites Conference on Composite Materials*.

[16] A. Parvizi, K. W. Garrett, and J. E. Bailey, "Constrained cracking in glass fibre-reinforced epoxy cross-ply laminates," *J. Mater. Sci.*, vol. 13, no. 1, pp. 195–201, 1978.

[17] Dassault Systèmes, *ABAQUS User's Manual*. 2011.

[18] M. L. Benzeggagh and M. Kenane, "Measurement of mixed-mode delamination fracture toughness of unidirectional glass/epoxy composites with mixed-mode bending apparatus," *Compos. Sci. Technol.*, vol. 56, no. 4, pp. 439–449, 1996.

[19] A. Turon, P. P. Camanho, and J. Costa, "An engineering solution for mesh size effects in the simulation of delamination using cohesive zone models," *Eng. Fract. Mech.*, vol. 74, pp. 1665–1682, 2007.

[20] A. Turon, P. P. Camanho, J. Costa, and J. Renart, "Accurate simulation of delamination growth under mixed-mode loading using cohesive elements : Definition of interlaminar strengths and elastic stiffness," *Compos. Struct.*, vol. 92, no. 8, pp. 1857–1864, 2010.

[21] P. Camanho, C. Dávila, and M. de Moura, "Numerical Simulation of Mixed-mode Progressive Delamination in Composite Materials," *Compos. Mater.*, vol. 37, no. 16, 2003.

[22] C. S. Lopes, P. P. Camanho, Z. Gürdal, P. Maimí, and E. V. González, "Low-velocity impact damage on dispersed stacking sequence laminates. Part II: Numerical simulations," *Compos. Sci. Technol.*, vol. 69, no. 7, pp. 937–947, 2009.